An experimental investigation of the stability of Poiseuille flow

By RICHARD J. LEITE
University of Michigan, Ann Arbor, Michigan

(Received 23 April 1958)

An axially symmetric laminar flow of air was established in a long smooth pipe. This flow was steady up to Reynolds numbers of about 20,000, the capacity of the system. Small, nearly axially, symmetric disturbances were superimposed by longitudinally oscillating a thin sleeve adjacent to the inner wall of the pipe. Hot-wire anemometer measurements consisting of radial and longitudinal traverses were made downstream of the sleeve. These measurements indicated that within the Reynolds number range investigated (up to 13,000), the flow is stable to small disturbances. In general, the radial distribution of disturbance amplitudes was not independent of distance downstream; while the disturbances, as generated, exhibited imperfect axial symmetry, the non-symmetric part decayed more rapidly than the symmetric part. Results were interpreted in such a way that rates of propagation and rates of decay of the disturbances could be compared with those given by a recent theoretical stability analysis. It was found that the rates of decay are predicted fairly satisfactorily by the theory; however, the rates of propagation are not. In addition, it was found that transition to turbulent flow occurs whenever the amplitude of the disturbance exceeds a threshold value which decreases with increasing Reynolds number. Due to the departures from axial symmetry in the amplitude of the disturbance, it was not possible to obtain a quantitative measure of the threshold. A mathematical idealization of the disturbances, believed to be more akin to experimental perturbations than the classical model used in small-perturbation analyses, is proposed.

1. Introduction

The purpose of the experimental work reported here was to study the initial stability of Poiseuille flows. More precisely the intent was to determine the evolution in time of small controlled disturbances in the laminar velocity profile.

In the early work following Reynolds's investigations, it was observed (see, for instance, Prandtl & Tietjens 1934) that the Reynolds number of transition could be made to increase apparently without bounds if great attention was paid not to disturb the laminar flow upstream of the pipe. This indicated clearly that the initial state of the laminar flow bears on the transition process. While many experiments have contributed in other ways to an understanding of transition (see, in particular, Rotta (1956); and Webb & Harrington (1956)), no measurements have been reported on the manner in which a smooth laminar

regime amplifies or damps small residual disturbances which are unavoidably present in any flow.

On the other hand, small-disturbance stability theory has been applied several times to Poiseuille flow (e.g. Sexl 1927*a*, *b*; Pretsch 1941; Pekeris 1946). Neither the rigour nor the generality of these efforts have been universally granted. But all the analyses produced so far have concluded that axially symmetric Poiseuille flow is stable. A renewed interest in the theoretical aspects of the problem (Corcos 1952) led to the experimental work reported presently.

We might expect to learn from an experiment whether small disturbances are always damped or sometimes amplified in Poiseuille flows. Then we might wish to go beyond this purely qualitative consideration and describe the decay or amplification of a disturbance in time. To do this practically we should first classify our disturbances in some systematic way; for a disturbance is in general a three-dimentional vector function of x, y, z and t. It can be viewed more profitably as the synthesis of a large number of more elementary disturbances each of which can be characterized in time and space by a finite number of parameters. This is a point of view peculiar to small (i.e. linear) perturbation analysis which can be exploited both by theory and experiment. Unfortunately, what has been chosen traditionally as an elementary disturbance in the theoretical analysis of the problem is not what the experimenter would regard as simple. For Poiseuille flows, disturbances have been assumed to be axially symmetric (Sexl 1927*a*) and such that their stream function is given by

$$\Psi = \phi(r)\, e^{i\alpha(x-ct)}, \tag{1}$$

where α is real and c is complex.

Such a disturbance would have to be imposed at an initial instant everywhere in the pipe and, in particular, periodically in the axial direction—a requirement which was judged impracticable. The elementary disturbances generated in the pipe for the experiment reported presently were, of necessity, of a different kind. They were induced along a short length of the pipe wall and they were periodical in time. By traversing the pipe downstream of the disturbance generator in the radial and the axial direction and along different azimuths, it was possible to measure the amplitude distribution of the disturbances, and, by comparing the instantaneous signal at various points, to establish the phase relationship between neighbouring points. Thus, the space description of the disturbance at a given time was recorded, together with the frequency at which this pattern was sinusoidally varied in time.

A description of the experimental apparatus and procedure is given first. The results are then summarized and discussed. Some attention is paid to a comparison with the results of a recent analysis. Finally, a few observations are reported on the behaviour of larger periodic disturbances.

2. Experimentation

Apparatus

Experiments were conducted in a horizontal Lucite pipe, 1·25 in. in diameter and 73 ft. (700 diameters) long. Figure 1 is a schematic diagram of the equipment. High-pressure air (90 lb./in.^{2}) from the laboratory supply line was passed

through a separator to remove most of the oil and water present in the incoming air. From the separator, the air proceeded through an activated alumina dryer to a pressure-regulating valve which controlled the pressure in a 100 cu.ft. storage tank used as a constant pressure source for the air supply system. Air flowed from the tank through a flow meter to the settling chamber and thence through a smooth contraction into the pipe.

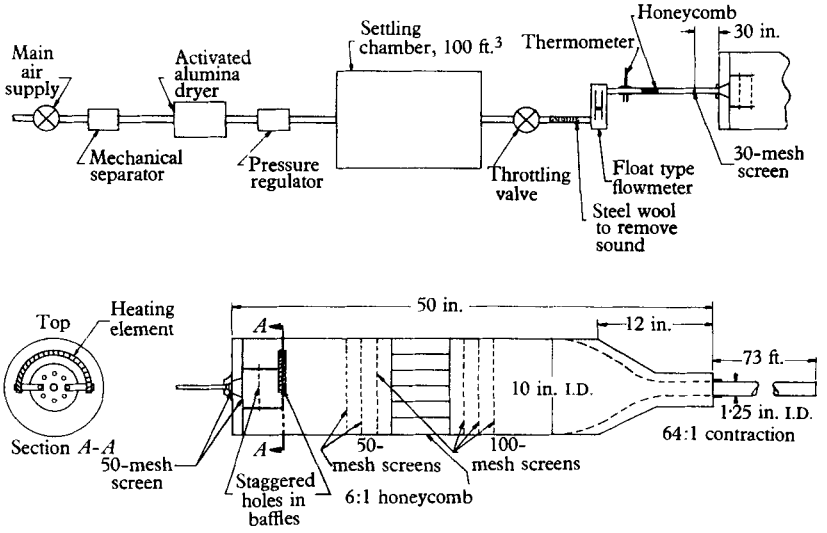

FIGURE 1. Schematic diagram of air supply system.

Uniformity of the internal diameter and concentricity of the pipe, as supplied by the manufacturer, were found to be within 0·005 in. for all sections of the pipe. The length of each section was approximately 50 in. To eliminate any adverse effects due to curvature along the length of the pipe, a theodolite was used to align and level the pipe. This method of alignment resulted in a system which departed at most only a few hundredths of an inch from true alignment over the entire length of the pipe.

The capacity of the laboratory air supply allowed operation at a maximum Reynolds number of approximately 20,000. No natural transition to turbulent flow was observed up to that Reynolds number. However, the supply pressure varied widely for the higher flow rates and therefore stability measurements were not attempted beyond a Reynolds number of 13,000.

All measurements were made with a hot-wire anemometer by conventional methods. In order to limit the size of the probe, only a U-meter was used. The wires were calibrated in a free jet. Figure 2 (plate 1) shows a typical hot-wire probe assembly used to make radial surveys inside the pipe. The hot-wire probe was accurately positioned in the radial direction by a micrometer gauge to which the probe was attached. The azimuth of the probe could be changed by merely rotating the entire probe assembly about the axis of the pipe. The hot-wire element itself was a platinum wire (Wollaston process) approximately 0·04 in. in length and 0·0002 in. in diameter. It could be placed at any radial position, relative to the wall of the pipe, with an accuracy of 0·003 in.

To take measurements at various axial positions while keeping a fixed radial distance from the wall, a probe was constructed which could be made to slide along the wall of the pipe. This probe is shown in the foreground of figure 2 and was called the 'bug'. By means of the 'bug', measurements of signal amplitudes and phase angles could be made as a function of distance along the pipe.

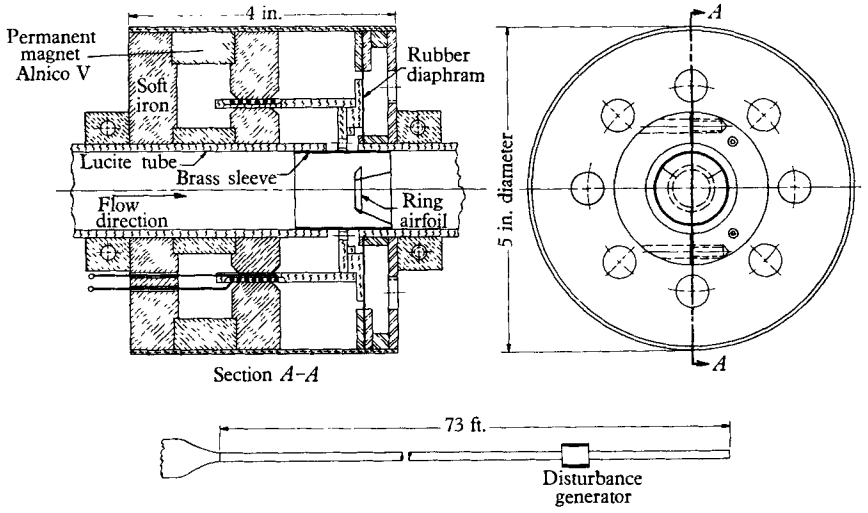

FIGURE 3. Schematic diagram of disturbance generator.

The disturbance generator was an electro-magnetic transducer which introduced velocity fluctuations of controllable amplitude and frequency into the flow within the pipe. Figure 3 is a schematic cross-section of the generator. The moving element was a thin (0·002 in.) cylindrical sleeve which lined the inner wall of the pipe over a length of 2 in. and was mounted concentrically to a coil located in a permanent magnetic field. An alternating current from a sinusoidal oscillator excited the coil and drove both coil and sleeve in longitudinal oscillations. The motion of the sleeve altered the boundary conditions at the wall and superimposed disturbance velocities upon the axially symmetric parabolic flow field.

Another means of generating axially symmetric disturbances, suitable for larger amplitudes, was to mount a ring airfoil within the cylindrical sleeve (see figure 3). The airfoil had a chord of 0·10 in. and a thickness of 0·003 in. The ring had a diameter of approximately 0·9 in. and was formed by truncating a cone having an apex angle of 6°.

Procedure

The laminar velocity profile of the undisturbed flow was checked before each series of disturbance measurements. Upon satisfactorily establishing that the mean flow was axially symmetric and parabolic, preliminary surveys were made to determine the range of disturbance frequencies which appeared least stable, i.e. those which decayed least with downstream distance. Then radial and longitudinal surveys of the disturbances were made downstream of the disturbance generator and at various azimuth angles.

A stationary hot-wire probe was used to observe any variation in the characteristics of the disturbance during each series of stability measurements. The ideal location for this probe would have been immediately downstream of the disturbance generator. However, since the wake of the probe would have greatly interfered with the disturbance, it was located instead in the test region diametrically opposite the test probe.

The hot wire was operated at a constant mean temperature. The mean square values of the disturbance amplitude were read on a millivoltmeter which was driven by a thermocouple attached to the output of the hot-wire voltage amplifier. Relative phase angles of the disturbance were determined as a function of radial and longitudinal separation distance by means of a dual beam cathode-ray oscilloscope. By applying the input voltage to the disturbance generator on one beam of the oscilloscope and the hot-wire signals on the other beam, relative phase angles of the disturbance velocities could be determined with an accuracy of approximately plus or minus five degrees.

Undisturbed pipe flow

(A) *The parabolic profile*

The velocity distribution of a steady laminar flow through a pipe, sufficiently far downstream of the entrance, is the well-known axially symmetric parabolic velocity profile of Poiseuille. When this profile was measured, deviation from axial symmetry was found throughout the pipe. The maximum velocity was not found to be on the geometric axis, the distribution being skewed as shown in figure 4. Radial surveys taken slightly downstream of the pipe inlet indicated that the asymmetry probably originated in the settling chamber; for the velocity of the core was not found to be uniform but slightly greater near the bottom of the pipe. Radial surveys of temperature and velocity were made within the settling chamber. However, the variation of these quantities was so minute that the results were inconclusive.

A systematic reorientation of the various components of the settling chamber and a modification of the settling chamber inlet failed to affect the pipe velocity profile. The conclusion was reached that the configuration of the settling chamber was not to blame and that the trouble was thermal rather than geometrical.

In order to combat distortions due to thermal effects, a heat source consisting of a nichrome wire wound on a curved glass tube, which spanned an arc of approximately 150°, was placed at the upstream end of the settling chamber (see figure 1). By varying the heating current supplied to this element, one could fix the location of the maximum in the velocity profile, far downstream, above or below the centreline; added current displaced the profile upwards. The average amount of heat added was approximately 10 W; assuming that half of the air passing through the settling chamber was heated uniformly, the total temperature rise would have been 2·3 °C at $R = 13{,}000$. The amount of heating current necessary was found to be an increasing function of the room temperature, which undoubtedly influenced the temperature of the air in the storage tank. It also depended somewhat on the Reynolds number.

Thereafter, this method of improving the velocity profile in the pipe was used. Prior to conducting stability measurements, velocity profiles were measured at the stations where the experiments were to be conducted, and the heating current was adjusted as required. Typical examples of velocity profiles with and without heat added are shown in figure 4.

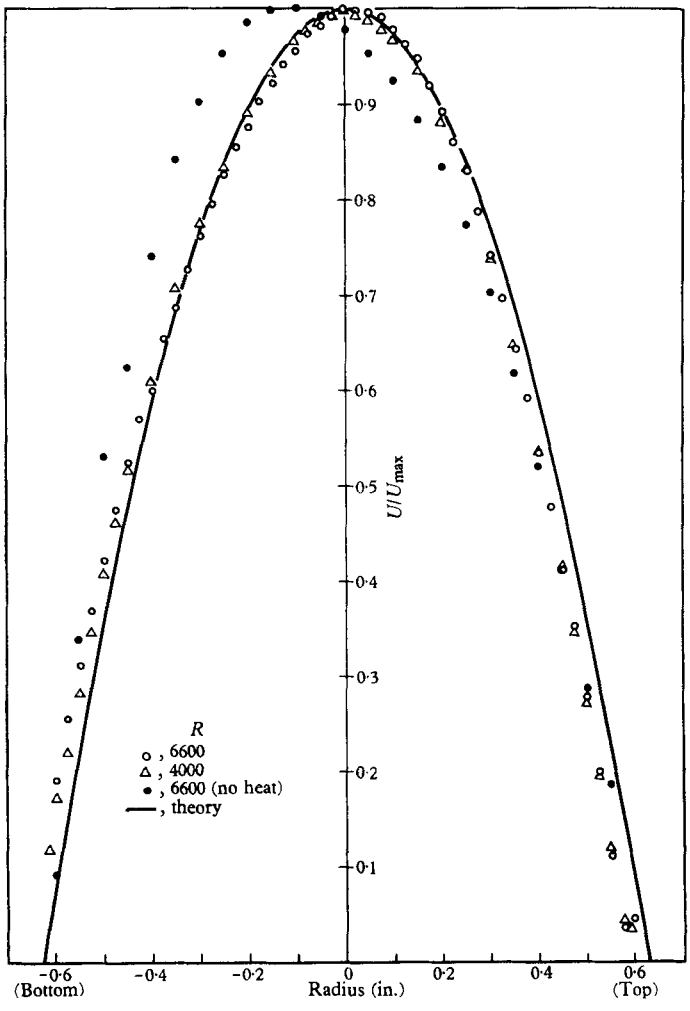

FIGURE 4. Mean velocity profiles, $R = 4000$ and 6600.

(B) *Residual unsteadiness*

Small residual disturbances were found to provide a noise background in the flow. The mean amplitude of their axial component u'/U was measured. It had a maximum value of approximately 10^{-4}. These disturbances were believed to be largely caused by radiated sound, because their amplitudes varied little across the pipe.

(C) *The entrance flow*

Some velocity profiles were obtained at several Reynolds numbers in the laminar transition region of the pipe, where the entrance flow evolves into a fully-developed parabolic profile. These profiles were compared with the calculated results of Boussinesq (1891). Satisfactory agreement existed at the lower Reynolds numbers; however, at higher Reynolds numbers, the formula gave values for the length of the pipe required for the development of a parabolic profile which seemed to be too large. For instance, at $R = 13{,}000$, the required length for a satisfactory profile was only 0·8 times the predicted length.

The small discrepancies found between experimental and theoretical profiles near the walls were believed to be due to the interference between the hot-wire probe and the boundary. Regardless of the source, however, the discrepancies did not appear large enough to influence the results significantly.

3. Results and discussion

The small disturbances introduced by the periodic motion of the sliding sleeve decayed as they travelled downstream for all the Reynolds numbers at which the measurements were taken (i.e. up to $R = 13{,}000$). Larger disturbances introduced by the motion of the ring airfoil did not decay at all Reynolds numbers. The part of the investigation, relating to the dynamics of these larger disturbances, is taken up separately later. Presently the behaviour of the small disturbances is discussed.

The data offered below covers a rather narrow band of frequencies. Preliminary tests indicated that frequencies above 45 c/s were damped so rapidly that accurate measurements could not be taken, while frequencies below 25 c/s caused difficulties related to the power requirements and to trace synchronization on the scope. Qualitative tests were made at frequencies ranging from 2 to 15 c/s. The disturbances at these frequencies always decayed as they proceeded downstream.

Axial symmetry

While axial symmetry was attempted both for the mean flow and for the disturbances, the disturbance amplitude recorded and shown in figure 5 is not independent of azimuth angle. This departure from axial symmetry could be caused by a number of factors such as small deviations of the fully developed flow from axial symmetry, small leaks around the disturbance generator allowing the generator to pump when in motion, and imperfections in the shape of the sleeve.

While departures from axial symmetry somewhat complicated the measurements, they lent greater generality to the results. In particular, it appears from figure 5 that the disturbances become more, or at least no less, axially symmetric as they proceed downstream. Thus, if one considers the perturbations to be the sum of an axially symmetric and a non-axially symmetric part, it appears that the latter decays at a faster rate than the former, as it proceeds downstream,

so that at least for the kind of disturbance tested the assumption of axial symmetry (as it is used in theoretical treatments of the problem) is not unreasonably restrictive.

General features of the disturbances

The peripheral surveys, which were used to determine the degree of axial symmetry of the disturbances, appeared to indicate that the disturbances possessed the same general character, as a function of azimuth angle, at each streamwise station. This fact supported previous measurements which indicated the absence of swirl in the pipe.

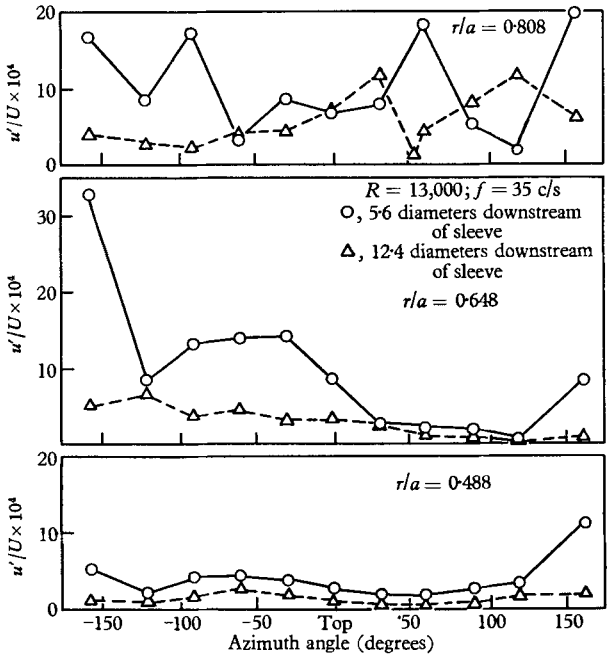

FIGURE 5. Peripheral distribution of amplitude of disturbances, $R = 13{,}000$.

Typical radial distributions of disturbance amplitude are given in figures 6 and 7. These disturbances seem to have, on the whole, the same shape except near the wall where a second amplitude peak occurs in some cases.

Inspection of the r.m.s. amplitude curve reveals that the u' component of the disturbance velocity approaches zero not only at $r = a$ (as is required by the no-slip condition at the wall) but also at $r = 0$. There seems to be no *a priori* reason to expect this result.

The amplitude curves also indicate that the amplitude of u' is a somewhat different function of r for different downstream distances. In general, the peak amplitude moves inwards as the disturbance propagates downstream. Figure 7 shows that the peak amplitude approaches an equilibrium position, but it is doubtful that similarity is really achieved before the disturbance is dissipated.

Radial variation of phase angle is given for several downstream distances in figures 8 and 9. The reference signal was measured at a different downstream station for each radial survey because of mutual interference of the two probes, hence, direct comparison between phase angles, at fixed radii for different stations, could not be made. However, 'bug' measurements, together with the driving voltage supplied to the disturbance generator, were used to establish

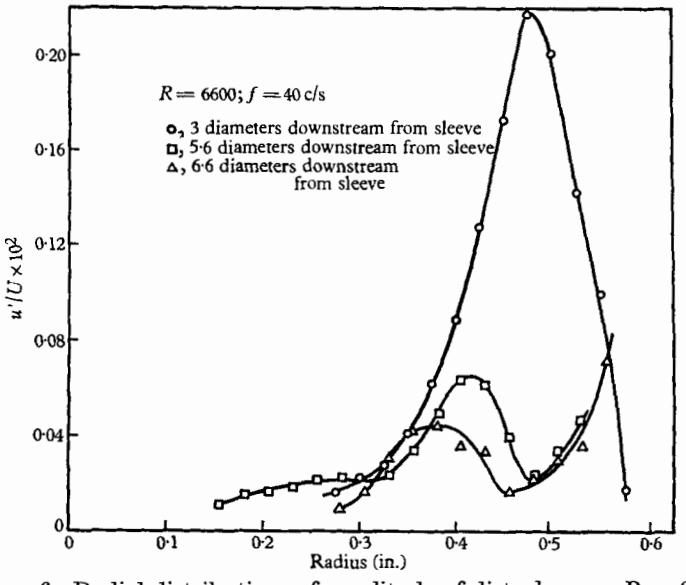

FIGURE 6. Radial distributions of amplitude of disturbances, $R = 6600$.

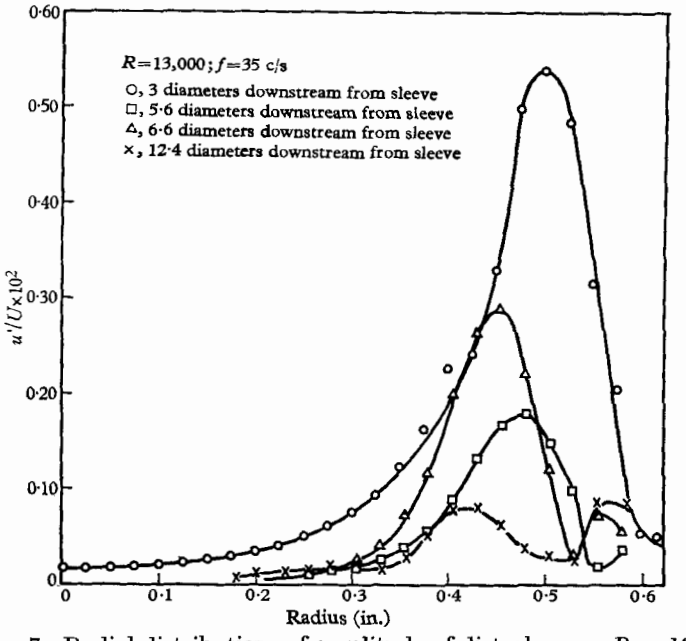

FIGURE 7. Radial distributions of amplitude of disturbances, $R = 13{,}000$.

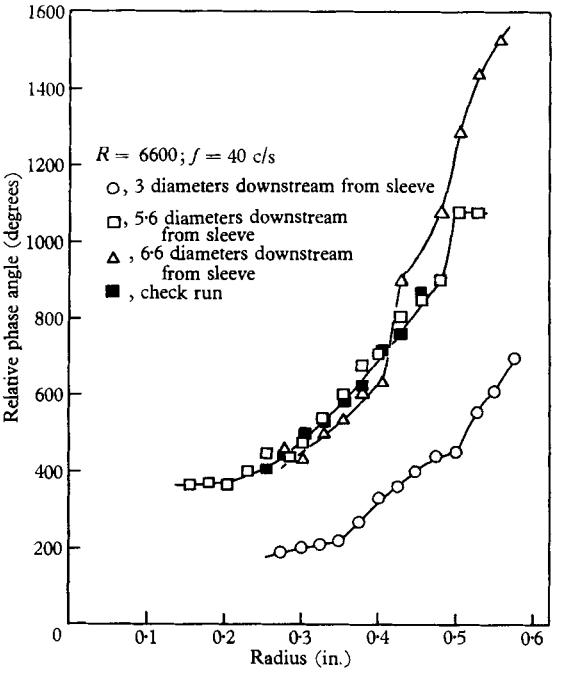

FIGURE 8. Radial distributions of phase angles of disturbances, $R = 6600$.

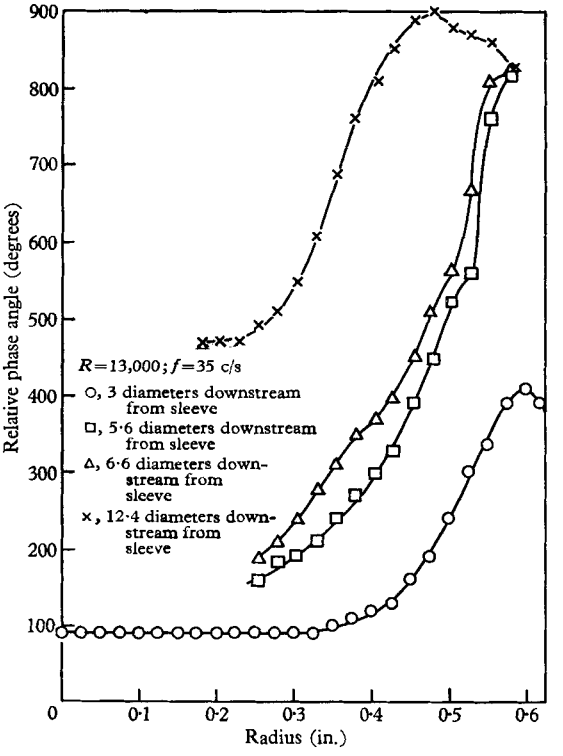

FIGURE 9. Radial distributions of phase angles of disturbances, $R = 13{,}000$.

longitudinal phase distributions of the reference probe at fixed radial positions. Therefore, by adjusting the radial-survey phase measurements, in such a manner that they corresponded with the 'bug' measurements, at prescribed radii, the actual radial phase distribution at each station was recorded. Typical results are shown in figures 8 and 9. From these curves, it appears that there is an inward convection of the disturbances, and that at least in first approximation the convection velocity depends little upon r and therefore little on the local stream velocity.

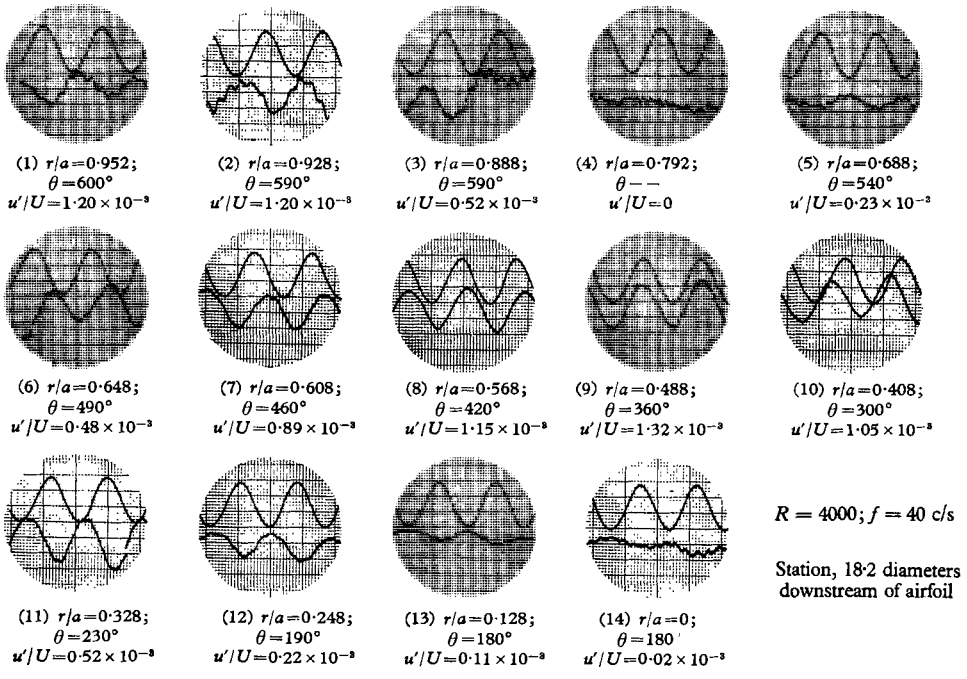

FIGURE 10. Radial distribution of disturbances (pictorial), $R = 4000$.

Several of the curves (see figures 6 and 8, 7 and 9) show a rather abrupt phase shift of approximately 180°. The corresponding amplitude curves reveal that a velocity minimum occurs at the same radial position. A torroidal vortex would betray its presence in just such a way. It would, however, exhibit no phase shift except at its centre where the amplitude is nil. In our case, the disturbance is somewhat more complex. It appears first near the wall and then propagates radially inwards.

Figure 10 reproduces the traces which appeared on the dual-beam cathode-ray oscilloscope during a typical radial survey. The top trace represents the driving voltage supplied to the disturbance generator. This signal provided a common reference for all phase-angle measurements. The time scale runs left to right. The relative amplitude of the disturbance is indicated at each radial position. These pictures illustrate that the signal phase lags as r decreases, and they give an example of a null occurring at $r/a = 0{\cdot}792$, together with a phase shift of approximately 180°.

Longitudinal surveys yielded rates of decay of the amplitude with x. These measurements, made with the 'bug', were quite sensitive to small orientation errors of the probe and great care had to attend them. Figure 11 shows, on the assumption that the decay in x is exponential, that there are two distinct rates of decay. The first one is believed to be associated with the radial redistribution of the disturbance amplitude and the second one with the characteristics of reasonably general disturbance profiles.

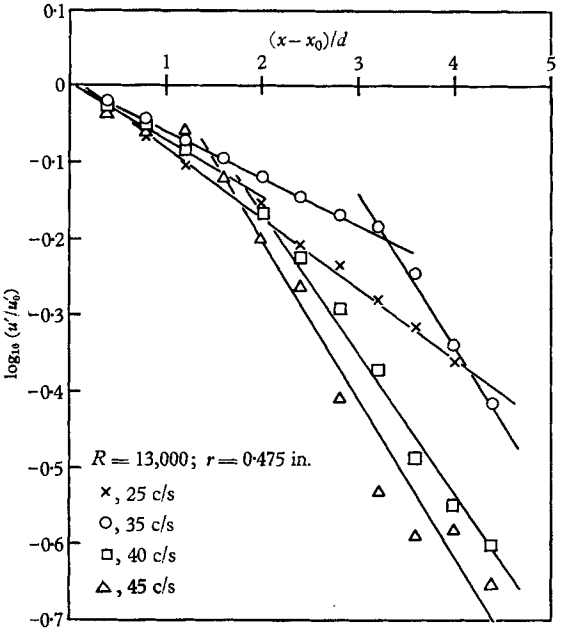

FIGURE 11. Decay of u-component of disturbances, $R = 13{,}000$.

The comparison of the phase angles of the signal, at various x-wide stations, with that of a reference signal at a fixed but arbitrary position (figure 12) supports the view that the disturbances are convected downstream at a rate which is independent of x.

An idealization of the experimental disturbances

In the Introduction it was noted that the disturbances generated for the experiment reported presently were unavoidably different from the elementary disturbances assumed in the linear perturbation theory. It can be seen from figures 6 and 7 that in the experiment the disturbance amplitude is far from homogeneous in the x-direction. Since, in fact, the disturbance amplitude decays largely in one wavelength, it is natural to suspect that an x-wise homogeneous representation might be seriously unrealistic. We have seen that, in view of the data, the assumptions of axial symmetry and of constant convective speed were not too restrictive. In addition, if one neglects the initial radial readjustment of disturbances, the assumption of radial similarity would seem

tolerable. In view of these facts a first-order description of the experimental disturbances generated in the present experiment might be

$$\Psi = \phi(r)\, e^{-\nu x + i\omega t},$$

where ν is complex and ω is real. This is the stream function of a disturbance periodic as well as exponential in x and periodic in t. It is clear that such disturbances lend themselves to small perturbation analysis, since they were formally

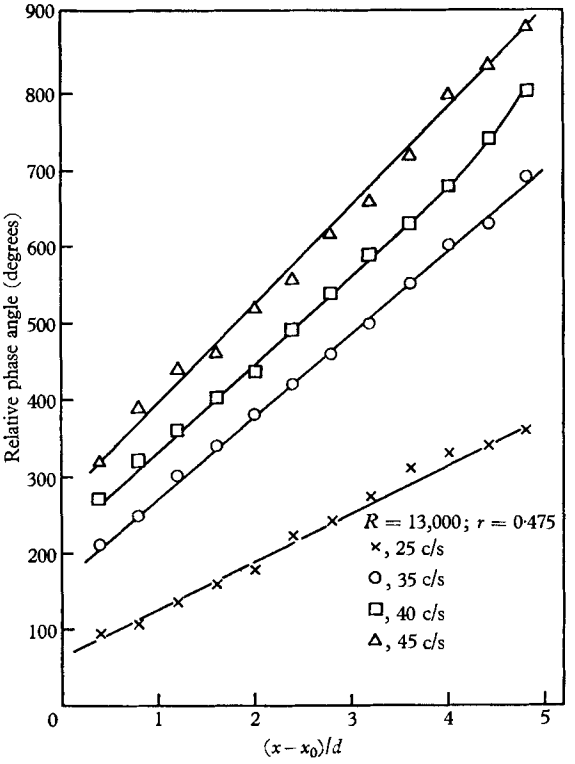

FIGURE 12. Longitudinal distributions of phase angles of disturbances, R = 13,000.

identical to the disturbances which satisfy the Orr–Sommerfeld equation (or rather the corresponding equations for fully developed pipe flow). The analysis would define the dependence of the real and imaginary part of ν (the x-rate of decay and the wavelength, respectively) on the frequency ω and the Reynolds number. Such quantities would be more directly comparable to those measured here. However, it was thought of interest to attempt a comparison of the present results with those of the recent theoretical analysis due to Corcos & Sellars (1959). In particular, in view of the fact that the disturbances are convected downstream at a uniform rate, it is possible to compare the measured convection-speeds with those of the theory. In addition, one may consider the rates of decay in x as time rates of decay for an observer travelling with the disturbances. Accordingly, the values of the damping factor c_i were obtained from the slopes of curves similar to those shown on figure 11.

From equation (1), the streamwise component of the velocity can be written

$$u = -\frac{\phi'(r)}{r} e^{\alpha c_i t} e^{i\alpha(x-c_r t)}. \tag{2}$$

Here c has been written $c = c_r + ic_i$.

The change in amplitude with respect to time can be expressed, using (2), as

$$\frac{u_2}{u_1} = \exp\left\{\int_{t_1}^{t_2} \alpha c_i \, dt\right\}. \tag{3}$$

In figure 11, x_0 corresponds to a station 3·6 diameters downstream from the sleeve. The r.m.s. amplitude of the disturbance velocity is u_0' at x_0 and u' at stations downstream of x_0.

Writing (3) in terms of the measured quantities, we get

$$\frac{u'}{u_0'} = \exp\left\{\int_{t(x_0)}^{t(x)} \alpha c_i \, dt\right\}$$

or

$$2{\cdot}3 \log_{10} \frac{u'}{u_0'} = \int_{t(x_0)}^{t(x)} \alpha c_i \, dt.$$

Differentiating with respect to t and using the relation $dx/dt = c_r$, this equation then becomes

$$c_i = \frac{2{\cdot}3 c_r}{\alpha} \frac{d}{dx}\left(\log_{10} \frac{u'}{u_0'}\right), \tag{4}$$

where $\alpha = 2\pi a/\lambda$. The non-dimensional wave velocities c_r were determined from curves similar to those shown in figure 12. The longitudinal distance the 'bug' had to be displaced to observe a 360° phase shift was called the wavelength λ of the disturbance. Then, by definition,

$$c_r = \frac{\lambda f}{U_{\max}}, \tag{5}$$

where f is the frequency of the disturbance and $U_{\max}$ is the maximum undisturbed stream velocity. Figure 13 compares both c_r and c_i with the values given by the theory of Corcos & Sellars (1959). The values of the propagation velocity c_r, which were deduced from the present measurements, are seen to be generally higher than those predicted by the theory for streamwise-homogeneous disturbances. On the other hand, the values of the damping factor given by the experiment agree rather well with the predictions of the theory. A fair amount of scatter appears in the measurements, in part because radial phase differences are large and a small amount of radial convection or readjustment introduces fairly large errors in apparent axial phase shift.

Ring airfoil: larger disturbances and transition

It has been shown above that small disturbances decayed at all Reynolds numbers investigated. Upon introducing the ring airfoil, disturbance amplitudes were increased appreciably and the stability characteristics of the flow changed markedly. At low Reynolds numbers comparison with theory is no longer possible and at higher Reynolds numbers the wake from the ring airfoil, when held stationary, was sufficient to cause transition to turbulent flow.

Results of measurements at a Reynolds number of 4000 are shown in figure 13. These results indicate that the larger disturbances propagate at a greater speed and decay more slowly than those generated by the sleeve and they stand far from results of the theory. Tests made at $R = 8000$ showed that transition was induced when the airfoil was oscillated with the smallest possible amplitude. At $R = 12{,}000$, with the airfoil held stationary, the induced disturbances were amplified, as they propagated downstream, with transition to fully turbulent flow finally resulting. A detailed description of this phase of the work was presented by Kuethe (1956).

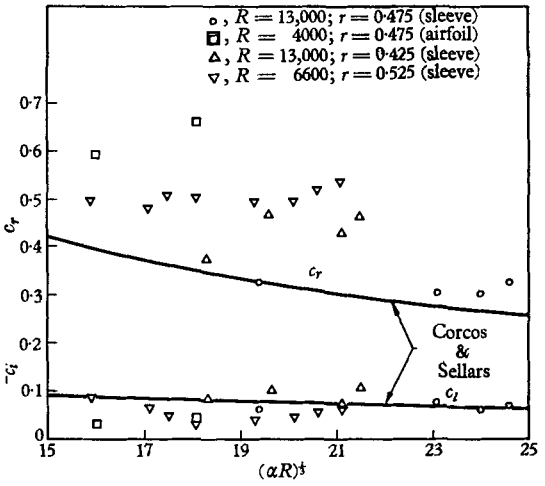

FIGURE 13. Comparison of experimental results with theoretical predictions; c_r and $-c_i$ *vs* $(\alpha R)^{\frac{1}{3}}$.

5. Conclusions

The following conclusions can be drawn from the present investigation.

1. Axially symmetric Poiseuille flow was found to damp the small disturbances introduced, whether they be axially symmetric or not, up to a Reynolds number of 13,000.

2. Experimental values of rate of decay were found to agree satisfactorily with those given by a recent theoretical analysis, even though assumptions of axial symmetry and longitudinal homogeneity of the disturbance are assumed in the latter.

3. To a first approximation, the propagation velocity of the disturbance does not depend upon radial position, hence upon local stream velocity, and is independent of distance downstream.

4. It has been found that small disturbances decay at all Reynolds numbers investigated and that large disturbances are unstable. Therefore, for fixed Reynolds numbers some disturbance of intermediate amplitude must be marginally stable.

The author is greatly indebted to Prof. Arnold M. Kuethe and Dr John R. Sellars for their advice, guidance and constructive criticism during the entire course of this work and to Dr Gilles M. Corcos for his helpful suggestions during

the preparation of the manuscript. This paper is based upon a dissertation submitted by the author to the University of Michigan in partial fulfilment of the requirements for the degree of Doctor of Philosophy. The work was sponsored, under the supervision of Prof. Kuethe, by the United States Air Force, through the Office of Scientific Research of the Air Research and Development Command under Contract No. AF 18(600)-350.

REFERENCES

BOUSSINESQ, J. 1891 *C.R. Acad. Sci., Paris*, **113**, 9 & 49.

CORCOS, G. M. 1952 *On the Stability of Poiseuille Flows*. Ph.D. Thesis, University of Michigan.

CORCOS, G. M. & SELLARS, J. R. 1959 *J. Fluid Mech.* **5**, 97.

KUETHE, A. M. 1956 *J. Aero. Sci.* **23**, 446.

PEKERIS, C. L. 1946 *Proc. Nat. Acad. Sci., Wash.*, **34**, 285.

PRANDTL, L. & TIETJENS, O. G. 1934 *Applied Hydro and Aero Mechanics*. New York: McGraw-Hill.

PRETSCH, J. 1941 *Z. angew. Math. Mech.* **21**, 204.

ROTTA, J. 1956 *Ing.-Archiv.* **24**, 4, 258.

SEXL, TH. 1927*a* *Ann. Phys., Lpz.*, **83**, 835.

SEXL, TH. 1927*b* *Ann. Phys., Lpz.*, **84**, 807.

WEBB, W. H. & HARRINGTON, R. P. 1956 *J. Aero. Sci.* **23**, 792.

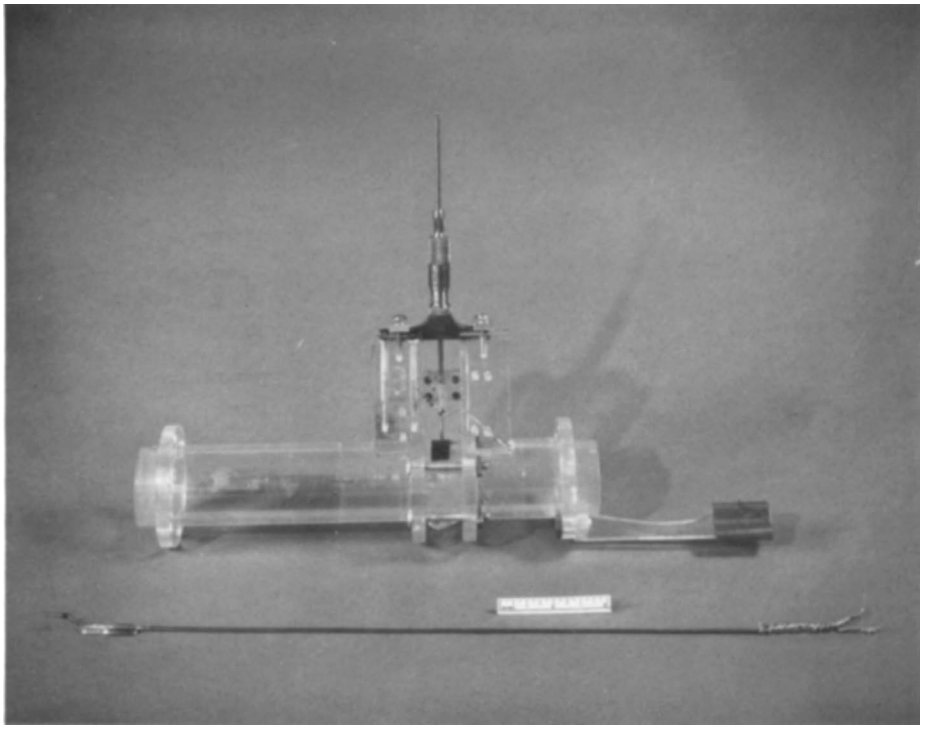

FIGURE 2 (plate 1). Photograph of hot-wire probe and 'bug'.

(*Facing p.* 96)